Title

The TY3 Gag3 Spacer Controls Intracellular Condensation and Uncoating

Journal

Journal of Virology, 85(7)

ISSN

0022-538X

Authors

Clemens, Kristina

Larsen, Liza

Zhang, Min

et al.

Publication Date

2011-04-01

DOI

10.1128/jvi.01055-10

JOURNAL OF VIROLOGY, Apr. 2011, p. 3055–3066 Vol. 85, No. 7
0022-538X/11/$12.00 doi:10.1128/JVI.01055-10

The TY3 Gag3 Spacer Controls Intracellular Condensation and Uncoating▽

Kristina Clemens,[1] Liza Larsen,[2] Min Zhang,[1]† Yurii Kuznetsov,[3] Virginia Bilanchone,[1] Arlo Randall,[4,5] Adam Harned,[6] Rhonda DaSilva,[6]‡ Kunio Nagashima,[6] Alexander McPherson,[2] Pierre Baldi,[3,4] and Suzanne Sandmeyer[1,2,3,4]*

Departments of Biological Chemistry,[1] Microbiology and Molecular Genetics,[2] Molecular Biology and Biochemistry,[3] and Computer Science,[4] and Institute for Genomics and Bioinformatics,[5] University of California, Irvine, California 92697, and Electron Microscope Laboratory, NCI-Frederick, SAIC-Frederick, Inc., Frederick, Maryland 21702[6]

Received 16 May 2010/Accepted 10 January 2011

Cells expressing the yeast retrotransposon Ty3 form concentrated foci of Ty3 proteins and RNA within which virus-like particle (VLP) assembly occurs. Gag3, the major structural protein of the Ty3 retrotransposon, is composed of capsid (CA), spacer (SP), and nucleocapsid (NC) domains analogous to retroviral domains. Unlike the known SP domains of retroviruses, Ty3 SP is highly acidic. The current studies investigated the role of this domain. Although deletion of Ty3 SP dramatically reduced retrotransposition, significant Gag3 processing and cDNA synthesis occurred. Mutations that interfered with cleavage at the SP-NC junction disrupted CA-SP processing, cDNA synthesis, and electron-dense core formation. Mutations that interfered with cleavage of CA-SP allowed cleavage of the SP-NC junction, production of electron-dense cores, and cDNA synthesis but blocked retrotransposition. A mutant in which acidic residues of SP were replaced with alanine failed to form both Gag3 foci and VLPs. We propose a speculative "spring" model for Gag3 during assembly. In the first phase during concentration of Gag3 into foci, intramolecular interactions between negatively charged SP and positively charged NC domains of Gag3 limit multimerization. In the second phase, the NC domain binds RNA, and the bound form is stabilized by intermolecular interactions with the SP domain. These interactions promote CA domain multimerization. In the third phase, a negatively charged SP domain destabilizes the remaining CA-SP shell for cDNA release.

Most retroviruses and some retrotransposons (collectively referred to as retroelements) have functionally analogous capsid (CA) and nucleic acid-binding domains contained within the major structural Gag precursor polyprotein (9, 40). In addition to these domains, some retroelement structural polyproteins contain short spacers (SP) that have been implicated in particle morphogenesis but which do not code for mature protein derivatives with known functions (Fig. 1A to C). For example, the Gag structural protein of human immunodeficiency virus type 1 (HIV-1) contains SP domains between nucleocapsid (NC) and p6 (SP2, also termed p1), and between CA and NC (SP1 or p2). Rous sarcoma virus (RSV) and bovine immunodeficiency virus (BIV) Gag polyproteins have SP domains between CA and NC. HIV-1 mutants in which SP1 is deleted fail to condense properly (23). In the case of the alpharetrovirus RSV, short insertion mutations in SP result in budding tubules rather than production of spherical viruses (19), and RSV Gag mutants lacking SP are noninfectious (7). Thus, the presence of SP contributes to particle assembly. SP domains have also been proposed to influence Gag interaction with RNA (14, 18, 38), multimerization and membrane association (12, 13), particle size (24), and Gag processing rate (31, 32).

Protease (PR)-mediated production of SP from Gag is an essential step in morphogenesis for retrovirus Gag proteins containing discrete SP domains. HIV-1 PR processing of Gag polyproteins is ordered, with SP1-NC cleavage first, followed by matrix (MA)-CA cleavage, and finally CA-SP1 cleavage. Mutations that block processing decrease production of infectious virus (34; reviewed in reference 9). The intermediate MA-CA cleavage produces the amino terminus of CA to form a salt bridge required for *in vitro* assembly of mature cones (44). However, *in vitro* systems have also shown that Gag derivatives having amino-terminal extensions of CA require a free CA carboxyl terminus to form cones (10, 33). Furthermore, disruption of HIV-1 CA-SP1 cleavage *in vivo* by mutation (1, 23) or chemical inhibition (28) blocks the transition from immature to condensed conical particles.

Comparisons of retrovirus SP domains between CA and NC domains reveal little conservation of either length or sequence (Fig. 1C). Furthermore, Gag sequences spanning the CA-NC junction are not well conserved, so it is possible that where SP does not exist, its functions have been acquired by other domains. For example, Moloney murine leukemia virus (MoMLV) lacks an SP domain at the CA-NC junction but contains a charged helix domain in the carboxyl-terminal domain of CA that is important for virus-like particle (VLP) assembly and size determination (6). Similarly, Mason-Pfizer monkey virus lacks a canonical SP domain but does have an

* Corresponding author. Mailing address: Department of Biological Chemistry, University of California, Irvine, Irvine CA 92697. Phone: (949) 824-7571. Fax: (949) 824-2688. E-mail: sbsandme@uci.edu.
† Present address: Department of Molecular and Medical Pharmacology, University of California, Los Angeles, CA 90095.
‡ Present address: Clinical Research Management, Office of Regulated Studies, United States Army Medical Research Institute of Infectious Diseases, Fort Detrick, MD 21702.
▽ Published ahead of print on 26 January 2011.

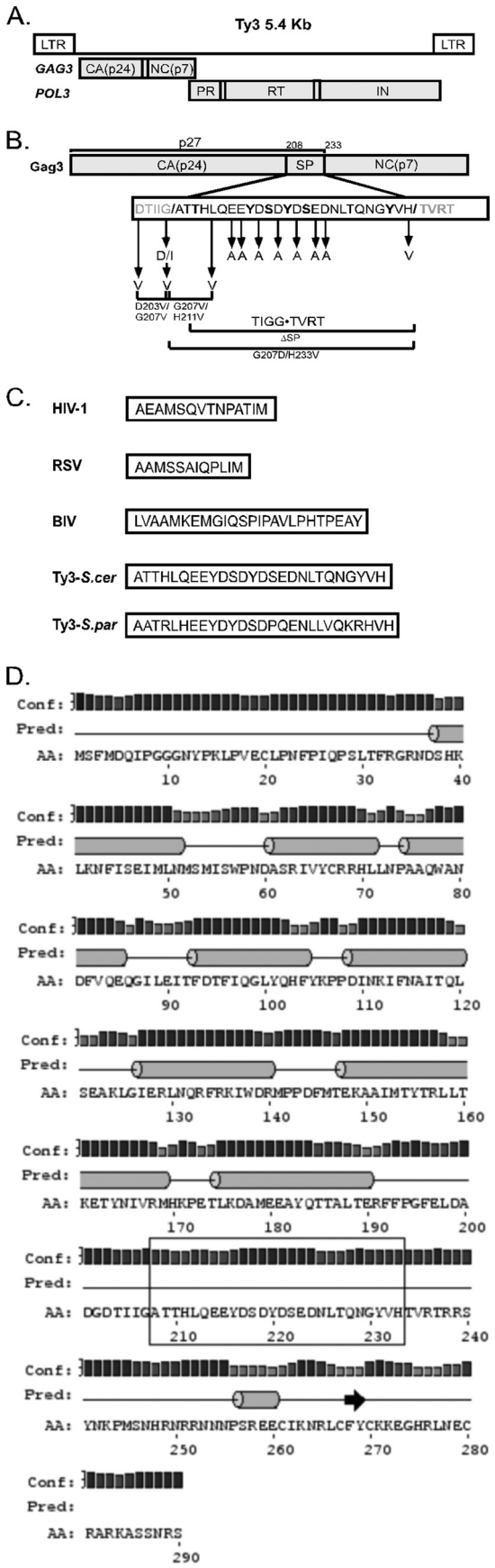

FIG. 1. Ty3 genome and spacer constructs. (A) Ty3 genome organization. (B) Ty3 Gag3 with CA, SP, and NC domains. Intermediate processing product CA-SP (p27) is indicated and spans amino acids 1 to 233. SP is comprised of residues 208 to 233. Boxed residues are the SP domain and C-terminal CA and N-terminal NC regions flanking SP. Processing sites between CA-SP and SP-NC are demarcated by slashes. Alanine scanning mutations were introduced at bolded residues that are potential phosphorylation targets. Mutations to block processing at CA-SP or SP-NC sites (G207D, G207I, and H233V) or to neutralize charged residues (D/E → A) are indicated by arrows. Double mutations designed to block CA-SP processing, to concomitantly block processing at the CA-SP and SP-NC sites, or to delete the SP domain (ΔSP) are indicated by brackets. (C)The amino acid sequences of retrovirus and retrotransposon SP domains at the CA-NC domain junction of Gag polyprotein. Amino acid sequences of the retroviral SP domains were obtained from the following references: HIV-1, Krausslich et al. (23); RSV, Craven et al. (7); BIV, Guo et al. (11); Ty3, Kuznetsov et al. (25); and $Ty3_{Sp}$, Fingerman et al. (8). (D) Secondary structure of Ty3 Gag3 predicted by the PSIPRED server using default parameters. Predicted helices are shown as cylinders, and the predicted strand is shown as an arrow. The prediction confidence at each position is represented by a vertical bar, where the bar height corresponds to the prediction confidence. The SP domain is boxed. Note that the SP domain is predicted to contain no regular secondary structure. AA, amino acids.

amino-terminal domain of NC that contributes to particle assembly (4, 37).

The budding yeast long terminal repeat (LTR) retrotransposon Ty3 (Fig. 1A) contains *GAG3* and *POL3* overlapping open reading frames (ORFs) that encode CA, SP, and NC major structural proteins (*GAG3*) and PR, reverse transcriptase (RT), and integrase (IN) catalytic proteins (*POL3*) (39). Like most retrotransposons, Ty3 undergoes an intracellular replication cycle and lacks matrix and envelope (Env) domains necessary for extracellular steps in the retroviral life cycle. Expression of Ty3 results in production of RNA, Gag3, and Gag3-Pol3 polyproteins. Gag3 multimerizes with Gag3-Pol3 and associates with genomic RNA to form VLPs. These particles are distributed in size, with most between 32 and 52 nm in diameter (15, 25). After VLP formation, Ty3 PR processes itself from Gag3-Pol3, cleaves Gag3 precursor proteins into CA, SP, and NC (Fig. 1B), and further processes Gag3-Pol3 into RT and IN. Processing and maturation of the VLP occur at cleavage sites similar to those targeted by retroviral PR (21) and result in condensation of the RNA without the massive CA reorganization that occurs within the retrovirus envelope (25–27). Protein sequence analysis of mature Ty3 CA and NC proteins allowed inference of a 26-residue SP domain separating CA and NC (21, 25). Ty3 SP has seven Glu and Asp residues, making it highly negatively charged. In addition, it contains eight Thr, Ser, and Tyr residues which are potentially phosphorylated. Comparison of Ty3 to a *Saccharomyces paradoxus* Ty3 ($Ty3_{Sp}$), shows conservation of the acidic residues in SP although overall Gag and even SP sequences have diverged (Fig. 1C) (8).

To better understand the role of the SP domain in morphogenesis of a retrotransposon, Ty3 was mutagenized to interrupt processing and to delete SP or neutralize its charge. The results of these studies showed that SP is not essential for assembly of particles, and production of NC in the presence or absence of SP is sufficient for a significant amount of cDNA synthesis.

TABLE 1. Base plasmids

Plasmid	Description	Genetic marker(s)	Reference(s) or source
pGEM3z	Multiple-cloning region	Amp^r	Promega
pLZL2426	pGEM3z with Ty3 sequence nucleotides 123 to 2351	*URA3*, 2μm, Amp^r	27
pDLC201	Full-length Ty3; Gal inducible	*URA3*, 2μm, Amp^r	16, 27
pNB2361	*HIS3*-marked full-length Ty3; Gal inducible	*URA3*, *HIS3*, *ARS/CEN*, Amp^r	3
pPK689	Ty3 target integration site	*HIS3*, *ARS/CEN*, Amp^r	20

However, failure to process CA-SP or the absence of SP results in a retrotransposition defect at some step subsequent to cDNA synthesis. An SP mutant in which acidic residues were replaced with Ala failed to form intracellular foci and VLPs. Based on these observations, we speculate that SP functions as a molecular "spring" in which the negatively charged SP and positively charged NC domains of Gag3 first interact intramolecularly to limit multimerization and then interact intermolecularly to promote correct multimerization of Gag3 on genomic RNA. After proteolytic processing of NC and formation of the electron-dense ribonucleoprotein core, a negatively charged CA-SP intermediate could promote processing and uncoating.

MATERIALS AND METHODS

Strains and culture conditions for *Saccharomyces cerevisiae* and *Escherichia coli*. The *S. cerevisiae* strain yTM443 (*MAT***a** *ura3-52 trp1-H3 his3-Δ200 ade2-101 lys2-1 leu1-12 can1-100 bar1*::*hisG* Ty3 null) (30) was used unless otherwise specified. For transmission electron microscopy (TEM), the *S. cerevisiae* strain BY4741 (*MAT***a** *his3Δ1 leu2Δ0 met15Δ0 ura3Δ0*) was used. For the quantitative transposition assay, a derivative of BY4741, yVB1672 (*MAT***a** *his3Δ1 leu2Δ0 met15Δ0 ura3Δ0* yGR109W::*loxP* yIL080W::*loxP*), in which the two Ty3 elements located on chromosomes VII and IX were replaced with *loxP* sites, was utilized. *E. coli* strain DH5α [λ^- ϕ80*lacZ*ΔM15 Δ(*lacZYA-argF*)*U169 recA1 endA1 hsdR17*(r_{K^-} m_{K^+}) *phoA supE44 thi-1 gyrA96 relA1*] (Invitrogen, Carlsbad, CA) was used for cloning and plasmid preparation.

S. cerevisiae was grown in synthetic complete medium containing dextrose (SD), galactose (SG) at 2%, or raffinose (SR) at 1% (wt/vol) and lacking bases or amino acids as appropriate for selective conditions (3). For induction, cells were pregrown in SR medium to an optical density at 600 nm (OD_{600}) of approximately 0.3 and then induced with the addition of galactose to a final concentration of 2% and allowed to grow for times indicated in descriptions of specific experiments. *E. coli* cells were grown and transformed as previously described (27).

Plasmid construction and mutagenesis. Mutagenesis of Ty3 Gag3 was performed as previously described (27). Vectors and base plasmids for other constructs and mutagenesis are described in Table 1. Plasmid pLZL2426 containing a region within *GAG3* was used as a template for QuikChange mutagenesis, according to the manufacturer's protocol (Stratagene, Cedar Creek, TX). Complementary primers for mutagenesis of the Ty3 SP-coding region (see data at https://webfiles.uci.edu/sbsandme/lab/) were obtained from Integrated DNA Technologies (Coralville, IA). The sequence of the subcloned, mutated region was determined (Genewiz Sequencing, South Plainfield, NJ), and the KpnI/BamHI (New England BioLabs, Ipswich, MA)-digested fragment was swapped for the wild-type (wt) fragment in the galactose-inducible Ty3 expression plasmid pDLC201. The spacer deletion (ΔSP) and acidic charge mutations (D/E → A) were constructed by two-fragment PCR using primers containing the desired mutations and overlapping regions of the pDLC201 Ty3 expression plasmid sequence. PCR products were annealed at overlapping regions and amplified using primers complementary to 5′ and 3′ ends of the fragments. Products of these reactions were subcloned into the pGEM3z cloning vector and swapped into the wt Ty3 backbone as described above.

Transposition assays. Mutant Ty3 elements were assayed for the ability to transpose into a transfer DNA (tDNA)-containing target plasmid using a semiquantitative patch assay as described previously (20). The Ty3 expression plasmid was a high-copy-number plasmid based on pDLC201 and marked with *URA3*. The target plasmid was a low-copy-number plasmid, pPK689, marked with *HIS3*. The wt or mutant Ty3 expression plasmid was cotransformed with the target plasmid into yeast strain yTM443. Transformants were selected, patched to SD medium lacking Ura and His (SD Ura^- His^-), and grown for one additional day. Patches representing four independent transformants were replica plated to SG Ura^- His^- medium and maintained at 24°C to allow Ty3 expression. Ty3 transposition into the target plasmid results in activation of transcription of a suppressor tRNA gene and growth on SD Ade^- Lys^- medium. Transposition events were scored as the number of papillations relative to wt Ty3. For the quantitative transposition assay, the low-copy-number plasmid pNB2361, containing a galactose-inducible, *HIS3*-marked Ty3 element, was used. Mutations were introduced as described above, and transposition was monitored as described previously (17).

Western blot analysis of Ty3 protein expression. Ty3 protein expression was monitored by Western blot analysis of cells transformed with pDLC201-based Ty3 expression plasmids. Four independent transformants containing wt Ty3 expression plasmid pDLC201 or mutant derivatives were pregrown in SR medium to an OD_{600} of ~0.3 and induced by growth in SG medium for expression of Ty3 elements. Whole-cell extracts (WCE) were prepared and fractionated as described previously (27). Fractionated proteins were transferred to Immobilon-P membrane (Millipore Corp., Billerica, MA) for 40 min using a semidry transfer apparatus with a discontinuous buffer system (Bio-Rad Laboratories, Hercules CA). Membranes were blocked in 2.5% nonfat milk in 1× phosphate-buffered saline (PBS)–0.1% Tween and incubated with primary rabbit polyclonal antibodies against Ty3 CA (30), NC (15), or IN (30) diluted 1:10,000, 1:1,000, and 1:1,000, respectively. Primary mouse monoclonal antibody against yeast phosphoglycerate kinase 1 (Pgk1) (Molecular Probes-Invitrogen, Carlsbad, CA) was diluted 1:5,000 and used to monitor Pgk1 as a loading control. Proteins were visualized with horseradish peroxidase-conjugated secondary antibody using an ECL^+ Western blotting reagent kit according to the manufacturer's protocol (GE Healthcare UK, Ltd). An LAS-4000 Fuji Imaging system (Fujifilm Life Sciences) was used to detect protein bands, and Multigauge software was used for quantification. All measured bands were within the linear range of detection for the imaging system.

Southern blot analysis of Ty3 cDNA. Ty3 cDNA production was monitored by Southern blot analysis. Transformants were grown and induced as described above for Western blot analysis, except that cells were grown for 18 h in SG medium to allow optimal detection of cDNA. DNA was extracted and analyzed as described previously (27), except that 10 μg of DNA was restricted with BamHI prior to agarose gel electrophoresis. The membrane-bound DNA was hybridized according to the manufacturer's protocol (Millipore Corp., Billerica, MA) with a ^{32}P-labeled DNA probe specific to a 2.9-kb region of the Ty3 genome. Hybridization was quantified using a Personal FX Molecular Imager and Quantity One software (Bio-Rad Inc., Richmond, CA). The cDNA level was normalized to the level of the Ty3 expression plasmid (27).

Indirect immunofluorescence analysis of Gag3 focus formation. Cultures of yeast transformed with pDLC201-based Ty3 expression plasmids were grown as described above and induced by growth in SG medium for 6 h. Cells were processed as described previously (2). The primary antibody, anti-CA, was diluted 1:1,000. The secondary antibody was Alexa Fluor-488 (anti-rabbit fluorescein isothiocyanate [FITC]-conjugated fluorochrome) (Molecular Probes-Invitrogen, Carlsbad, CA). DAPI (4′, 6-diamidino-2-phenylindole) was used at a concentration of 1 μg/ml in PBS to visualize nuclei. Microscopy was carried out essentially as described previously (2, 26).

RNA nuclease protection assay. Cells transformed with wt and mutant pDLC201-based Ty3 expression plasmids were induced for Ty3 expression for 6 h. A total of 20 OD units of cells was harvested and subjected to extraction of RNA and protein under native conditions. Nuclease protection assays were performed with TurboNuclease (Accelagen, San Diego, CA) but otherwise as previously described (27, 29).

TEM. BY4741 transformants carrying wt or pDLC201-based mutant Ty3 expression plasmids were grown at 24°C in SR Ura^- medium to early log phase, induced by addition of galactose to a concentration of 2%, and maintained for

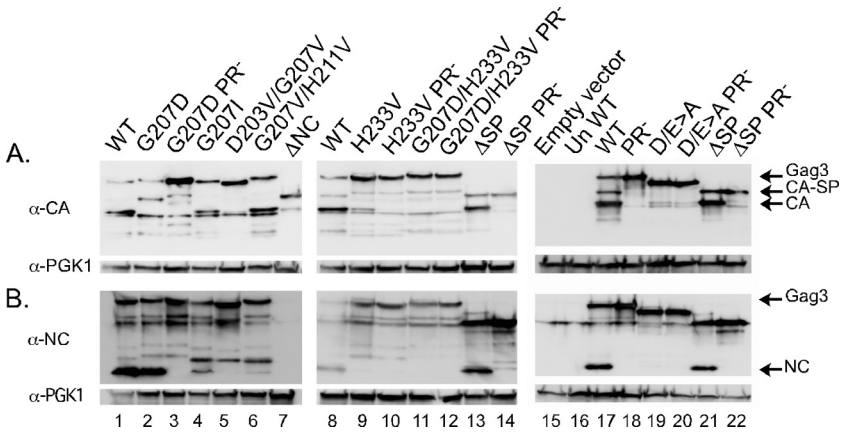

FIG. 2. Effect of SP mutations on Ty3 Gag3 processing. Yeast cells were induced for expression of wt or mutant Ty3 elements by growth in SG Ura$^-$ medium for 12 h. WCE were prepared, and 15 μg of total protein was fractionated on an SDS–4 to 20% polyacrylamide gradient gel. (A) Total protein from WCE probed with anti-CA antibody. (B) Total protein from WCE probed with anti-NC antibody. Eight Ala substitution mutants showed processing patterns similar to the pattern of wt Ty3 (data not shown). Pgk1 was monitored as a control for loading in blots of both panels. α, anti.

6 h. Western blot analysis was performed as described above to confirm Ty3 expression (data not shown), and cells were processed for transmission electron microscopy (TEM) as described previously (27, 43). A total of 100 cells of each transformant type were imaged with a transmission electron microscope (Hitachi H7600; Tokyo, Japan).

Preparation of VLPs for AFM. Yeast cells transformed with wt and mutant pDLC201-based expression plasmids were grown in SR medium at 24°C and used to inoculate 400 ml of SG medium. Cultures were grown for 18 h and 60 OD_{600} units of cells were harvested. VLPs were isolated by velocity sedimentation on sucrose step gradients using a modification of the previously described protocol (available at https://webfiles.uci.edu/sbsandme/lab/) and prepared for atomic force microscopy (AFM) analysis (25).

RESULTS

The lack of overall conservation between Ty3 and $Ty3_{Sp}$ SP (Fig. 1C) suggested that the role of SP might be to control separation of NC and CA species rather than to provide a specific structure. We first mutated residues at the SP junctions with the intent of disrupting production of specific Gag3 processing intermediates. We then examined the requirement for the distinctive negative charge of this domain.

Immunoblot analysis of Ty3 mutants disrupted in CA-SP and SP-NC processing. The Ty3 SP domain was defined by Edman degradation and mass spectrometry of flanking regions (25). Previous analysis of Ty3 PR processing sites showed that, similar to retrovirus PR cleavage sites, they are embedded in uncharged amino acids spanning P3 to P2′ residues (21). In the case of Ty3 SP, these contexts are IIG_{207}/AT and YVH_{233}/TV (where the slash indicates the cleavage position) (Fig. 1B). Analysis of Ty3 and retrovirus PR processing sites also suggested that beta-branched residues are excluded from the P1 position (21, 35) although this is not universal among retrovirus Gag processing sites (41). The pattern of wt Ty3 proteins detected by anti-CA showed full-length Gag3, an intermediate the size of the p27 CA-SP, and the 24-kDa CA, as well as other minor species (Fig. 2A, lane 1). The major proteins detected by anti-NC raised against an amino-terminal peptide (15) were full-length Gag3 and the mature, 7-kDa, 57-residue Ty3 NC (Fig. 2B, lane 1). To test the effect of disrupting SP processing on particle morphogenesis, the P1 residue at the CA-SP cleavage site was replaced with a beta-branched amino acid, creating mutant G207I. Extracts of cells expressing this mutant for 12 h were examined by Western blot analysis using anti-CA and anti-NC antibodies (Fig. 2A and B, lanes 4). Extracts showed increased unprocessed Gag3. However, rather than increased amounts of a p27 species, there were small amounts of CA. In addition, there was a species that reacted with the NC antibody but was larger than NC, potentially representing SP-NC. This suggested that the G207I mutation did not block CA-SP processing but, rather, enhanced production of an anomalous intermediate which could not be further processed.

Additional single and double mutations were introduced into Gag3 to more completely disrupt CA-SP processing. These included G207D, D203V G207V, and G207V H211V. G207D decreased amounts of both Gag3 and CA and resulted in elevated levels of a species with the expected mobility of CA-SP (Fig. 2A, lane 2). Disruption of PR processing by introduction of D59I in the PR active site (PR$^-$) (21) abolished this intermediate, indicating that it was a product of PR processing (Fig. 2A, lane 3). This species had the same mobility as a CA-SP species produced from an NC deletion mutant (ΔNC), supporting the interpretation that it was the CA-SP p27 precursor (Fig. 2A, lanes 2 and 7). Amounts of NC produced by the G207D mutant were similar to those produced by wt Ty3, indicating that the entire Gag3 was not likely to be misfolded and that NC production is independent of CA-SP processing (Fig. 2B, lane 2). Other mutations either abolished all apparent processing (D203V G207V) or, similar to G207I, allowed CA-SP cleavage but abolished production of NC (Fig. 2A and B, lanes 5 and 6). Retrotransposition of the G207D, G207I, D203V G207V, and G207V H211V mutants was not detectable using a qualitative genetic assay (Table 2).

In order to test the effect of disrupting processing at the SP-NC junction, the His residue at the SP-NC P1 position was replaced with the beta-branched amino acid Val (H233V) (Fig. 1B). This mutation eliminated production of NC and permitted production of only small amounts of CA (Fig. 2A and B, lanes 9). Introduction of the PR active site mutation into the H233V mutant did not

TABLE 2. SP mutant phenotypes

Mutation(s)	cDNA/plasmid ratio	IN[a]	Qualitative transposition score[c]	VLPs assembled[a]	Gag3 focus formation[a]	% RNA packaging
wt	1.000	+	+++	+	+	23.4 ± 10
T209A		+	+++			
T210A		+	+++			
Y216A		+	+++			
S218E		+	+++			
Y220A		+	+++			
S222E		+	+++			
S218E S222A		+	+++			
S218A S222E		+	+++			
S218E S222E		+	+++			
T227A		+	+++			
Y231A		+	+++			
G207D	2.400	+	None	+		
G207I	0.090	+[b]	None			
D203V G207V	0.001	−	None			
G207V H211V	0.050	+[b]	None			
H233V	0.280	+[b]	None	+		
G207D H233V	0.200	−[b]	None	+		
ΔSP	0.440	+	++	+	+	47.6 ± 5.0
D/E>A	0.010	−		−/+	−	4.3 ± 2.7
G207D PR$^-$		−		+		
H233V PR$^-$		−		+		
G207D H233V PR$^-$		−		+		
ΔSP PR$^-$	0.010	−		+	+	65.1 ± 8.8
D/E → A PR$^-$		−		−	−	1.9 ± 0.4

[a] The presence (+) or absence (−) of a feature is indicated.
[b] Integrase is present or absent with elevated minor cleavage products.
[c] +++ indicates the wild-type pattern.

significantly change the processing pattern (Fig. 2A and B, lanes 10). Thus, either H233V disrupts the Gag3 structure to an extent not compatible with recognition by PR, or SP maturation is ordered so that SP-NC processing creates the substrate for CA-SP processing. A mutant in which both processing sites were disrupted (G207D H233V) was also constructed. Western blot analysis of cells expressing this mutant with anti-CA and anti-NC antibody confirmed the anticipated absence of Gag3 processing species (Fig. 2A and B, lanes 11). Retrotransposition of the H233V and G207D H233V mutants was not detectable using the qualitative genetic assay (Table 2).

Overall, mutations at the SP-processing sites indicated that processing at both SP junctions was required for retrotransposition. Mutations that blocked processing at the amino-terminal SP junction did not block processing at the downstream SP-NC site. However, the mutation which interfered with processing at the carboxyl-terminal junction also disrupted amino-terminal junction processing. Although this could indicate that Gag3 folding was fundamentally disrupted, it could also be that processing at the ends of SP is ordered, with processing of SP-NC preceding processing of CA-SP.

Ty3 ΔSP assembles and undergoes proteolytic maturation. To test whether the Ty3 SP domain is essential for assembly of VLPs or for retrotransposition, the SP domain was deleted, creating a chimeric processing site ($IIG_{207}/T_{235}V$) at the synthetic CA-NC junction (Fig. 1B). This mutant was designated ΔSP. Western blot analysis of extracts from cells expressing ΔSP revealed a smaller Gag3 species that reacted with antibodies against CA and NC (Fig. 2A and B, lanes 13). However, the mutant Gag3 had an apparent mobility similar to that of the 27-kDa CA-SP, which was unexpected because full-length Gag3 is 34 kDa and SP is 3 kDa. Processed CA and NC species of the expected mobility were also detected, indicating that cleavage occurred at the chimeric site. To test the possibility that the unexpected species was an anomalous processing product, the PR catalytic site mutation was introduced into ΔSP, and the resulting mutant was analyzed (Fig. 2A and B, lanes 14). An elevated level of ΔSP PR$^-$ Gag3 with similar mobility to ΔSP Gag3 was observed. Although it is possible that this catalytically inactive chimeric protein could be cleaved by cellular proteases, Western blot analysis of cells induced for shorter time periods also displayed a Gag3 species of apparent mobility of 27 kDa (data not shown). These results argue that the detected species represents Gag3 and that, similar to what has been reported for the mobility of other proteins upon neutralization of negative charges, deletion of the negatively charged SP enhanced binding of SDS and increased relative mobility in SDS-PAGE by an amount disproportional to the decrease in molecular weight (MW) (46). Ty3 Gag3 processing is likely triggered, as with retroviral Gag maturation, during or subsequent to assembly (21, 27). Thus, correct processing of ΔSP Gag3 argues compellingly that this mutant assembles into a processing-competent species at a level comparable to that of wt Ty3 Gag3. Because this mutant appeared to correctly process Gag3 protein, retrotransposition was measured using both the qualitative genetic assay (Table 2) and a quantitative version of this assay (Table 3). The quantitative assay showed that retrotransposition was reduced by about 16-fold. Thus, deletion of the SP domain did not abrogate assembly but dramatically reduced retrotransposition.

Modeling based on cryo-electron tomography of the immature HIV-1 lattice predicted a bundle of SP alpha-helices span-

TABLE 3. Quantitative transposition of Ty3 SP mutants

Mutation(s)	Transposition frequency[b]	Fold decrease from wt
wt	$2.90 \times 10^{-3} \pm 0.39$	1
ΔSP	$0.18 \times 10^{-3} \pm 0.06$	16
ΔSP PR$^-$	$0.01 \times 10^{-3} \pm 0.00$	290
D/E → A	$<10^{-3}$	NA

[a] NA, not applicable.
[b] Frequency of cells that underwent transposition out of total cells plated.

ning the CA-SP boundary of HIV-1 Gag, which was proposed to contribute to HIV-1 Gag multimerization and particle assembly (47). However, PSIPRED modeling (5) does not predict an alpha-helical structure for Ty3 Gag3 SP (Fig. 1D). HIV-1 SP1 is proposed to act as a relatively independent structural element. Thus, if Ty3 SP and HIV-1 SP1 perform similar functions, it was possible that transposition of the Ty3 ΔSP mutant would be rescued by introduction of the HIV-1 SP1 domain. wt and PR$^-$ Ty3 elements in which SP1 replaced SP were constructed. The novel Gag species contained chimeric processing sites at the SP1 junctions. This construct produced and processed chimeric Gag3 protein and produced an amount of cDNA equivalent to 36% of the amount produced by wt Ty3. A quantitative assay showed that despite production of cDNA by the Ty3 HIV-1 SP1 mutant, it displayed a 50-fold-lower retrotransposition frequency than wt Ty3. The ΔSP mutant displayed only a 16-fold-lower transposition frequency than wt Ty3. Therefore, the substitution of HIV-1 SP1 did not rescue the Ty3 ΔSP mutant (data not shown).

Pol3 processing is not dependent upon Gag3 processing. Identification of mutations that blocked processing at one or both of the SP junctions allowed us to test whether processing of Gag3-Pol3 within the Pol3 domain is sensitive to the state of Gag3 maturation. This was assessed by Western blot analysis using anti-IN antibodies (Fig. 3A). Neither of the single mutations that disrupted SP production, G207D or H233V, disrupted production of mature IN (Fig. 3A, lanes 2 and 6). However, mutations with more severe effects, including G207I (Fig. 3A, lane 3) and G207V H211V (Fig. 3A, lane 5), which failed to produce NC but produced CA, and H233V (Fig. 3A, lane 6) and G207D H233V (Fig. 3A, lane 7), which failed to produce NC or CA, each produced a doublet of the approximate mobility (~100 kDa) of an RT-IN fusion in addition to IN. This species has been observed for wt Ty3 (22) although it was present in greater amounts in extracts of cells expressing these Gag3 processing mutants. Only in extracts of cells expressing the D203V G207V mutant was IN production undetectable (Fig. 3A, lane 4). wt levels of IN were also observed for the ΔSP mutant, indicating that the SP domain itself is not critical for production of IN from Gag3-Pol3 (Fig. 3A, lane 15). Because at least some mutations that affected production of CA and NC did not affect processing of IN from Gag3-Pol3, these results indicate that Gag3 processing products are unlikely to be required for processing of Gag3-Pol3. The D203V G207V mutations could have interfered with Gag3-Pol3 maturation and affected Gag3 folding or assembly and, therefore, only indirectly affected processing.

Charged residues, but not single, potentially phosphorylated residues, are essential for full-length Gag3 particle production. The ability of the ΔSP mutant to process precursor polyproteins (Fig. 2A and B, lanes 21, and 3A, lane 15), combined with the decrease in retrotransposition (Tables 2 and 3), suggested that SP is required downstream of proteolytic maturation. As noted above, this domain has a significant number of potentially phosphorylated and negatively charged residues, and the latter are conserved between Ty3 and $Ty3_{Sp}$. To test for an essential role of any single residue, each of the eight potential phosphorylation targets within the SP domain (Fig. 1B) was individually replaced with Ala. In addition, residues S218 and S222 were mutated to Glu to mimic phosphorylation. The resulting mutants were tested for expression and processing of Ty3 Gag3 by Western blot analysis. In all cases, amounts of CA and IN were similar to those produced by wt Ty3 (data not shown). Retrotransposition frequency of these mutants was also similar to that of the wt (Table 2). Correct protein processing and wt levels of retrotransposition indicated that particle assembly and cDNA synthesis occurred normally. Although these results do not exclude the possibility that phosphorylation contributes to SP function, they indicated that phosphorylation of any individual residue is not essential.

As discussed above, Ty3 SP contains a disproportionate number of acidic residues that would confer a high negative charge density. To test the contribution of this property, these residues were replaced with Ala (D/E → A). In order to distinguish any defects created by PR-mediated destabilization from assembly defects, the PR catalytic site mutation was introduced into this mutant (D/E → A PR$^-$). Cells expressing these mutants were examined for protein production and processing using antibodies against CA, NC, and IN. Extracts analyzed for CA and NC production showed that both mutants produced greater than wt levels of Gag3, but Gag3 processing

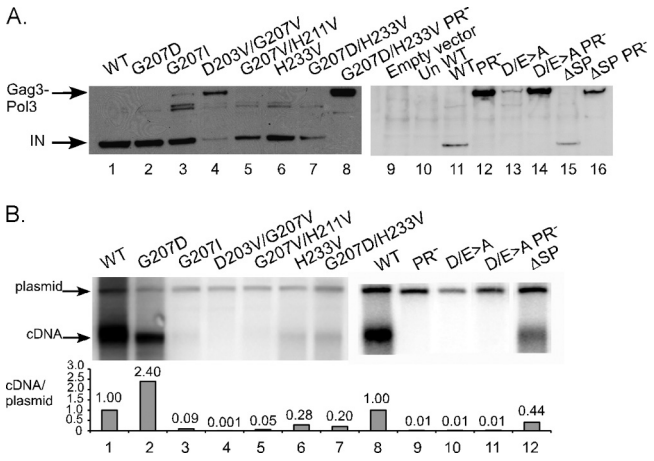

FIG. 3. Effect of SP mutations on Gag3-Pol3 processing and cDNA synthesis. (A) Western blot analysis of IN protein processed from Gag3-Pol3. Yeast cells were induced for expression of wt Ty3 or mutant derivatives and monitored for protein expression as described for Fig. 2 except that WCE were probed with anti-IN antibody. (B) Southern blot analysis of Ty3 cDNA. Transformants expressing wt and mutant Ty3 were grown in SG Ura$^-$ medium for 18 h. Extracted DNA was digested with BamHI to linearize the Ty3 plasmid. A ^{32}P-labeled probe to a 2.9-kb internal region of Ty3 was used to visualize Ty3 cDNA (5.4 kb) and the expression plasmid. The ratio of wt cDNA to plasmid signals was set to 1.0, and other samples were normalized to this value. Measurements are representative of two or more independent transformants tested.

products were not detected (Fig. 2A and B, lanes 19 and 20). Both D/E → A mutant Gag3 and the D/E → A PR$^-$ mutant Gag3 showed greater mobility than wt Gag3, consistent with the previous conclusion that the anomalous mobility of ΔSP relative to Gag3 is due to the reduction in negative charge. Western analysis using the anti-IN did not detect IN and detected only low levels of Gag3-Pol3 (Fig. 3A, lane 13). However, the PR$^-$ mutation restored the level of Gag3-Pol3 to that observed for wt Ty3 (Fig. 3A, lane 14). These results are most consistent with aberrant assembly, sufficient to activate PR, but insufficient to generate a stable, replication-competent particle.

Processing of the NC domain from the SP domain is sufficient for cDNA synthesis. The proteolytic maturation observed for SP mutants suggested that a significant subset was assembly competent. However, retrotransposition was undetectable. In order to determine whether relatively subtle defects in processing could have more profound consequences for reverse transcription, cDNA production was examined. Cells were induced for 18 h to express wt and SP mutant Ty3 elements. DNA was extracted, and Southern blot analysis was performed using a Ty3-specific probe. Comparison of the ratio of extrachromosomal Ty3 cDNA to Ty3 donor plasmid in cells expressing wt and mutants (Fig. 3B) showed that the G207D mutant—the only processing mutant that generated wt levels of NC—produced a higher ratio of cDNA to plasmid than wt Ty3 (Fig. 3B, lane 2). Cells expressing mutants H233V and G207D H233V showed much lower ratios of cDNA to plasmid (Fig. 3B, lanes 6 and 7), and other processing site mutants did not produce detectable cDNA. The ΔSP mutant produced approximately half the ratio of cDNA to plasmid produced by wt Ty3 (Fig. 3B, lane 12). It was striking that the reduction in the amount of cDNA generated for G207D and ΔSP mutants was much less severe than the decrease in retrotransposition. The D/E → A mutant produced no cDNA, consistent with its failure to process Gag3 (Fig. 3B, lane 10). Thus, overall, levels of cDNA generated by a mutant correlated with the ability to generate mature NC.

The role of the negatively charged SP domain in focus formation and RNA packaging. The Gag3 processing and cDNA levels observed for the ΔSP mutant indicated that SP is dispensable for assembly and cDNA synthesis but is critical for some later step. However, the absence of D/E → A Gag3 processing raised the possibility that the charged residues in SP play a critical early role if SP is present. Cells induced for Ty3 expression form foci containing Ty3 Gag3 and Gag3-Pol3 and Ty3 RNA (2). Focus formation is one of the earliest correlates of assembly (26, 27). In order to gain insight into how SP might contribute to assembly, we examined the abilities of the D/E → A and ΔSP mutants and their PR$^-$ derivatives to form foci (Fig. 4A). Indirect immunofluorescence studies using antibodies to detect CA showed that cells expressing wt Ty3 displayed the characteristic one or two large foci, and PR$^-$ derivatives were similar, but with less diffuse cytoplasmic fluorescence. In contrast, cells expressing the D/E →A mutant had considerable cytoplasmic fluorescence, consistent with the Western blot analysis showing wt levels of Gag3. However, this fluorescence was diffuse, with many small speckles, and was not readily distinguishable from the D/E → A PR$^-$ derivative. Cells expressing ΔSP showed foci indistinguishable from those of cells

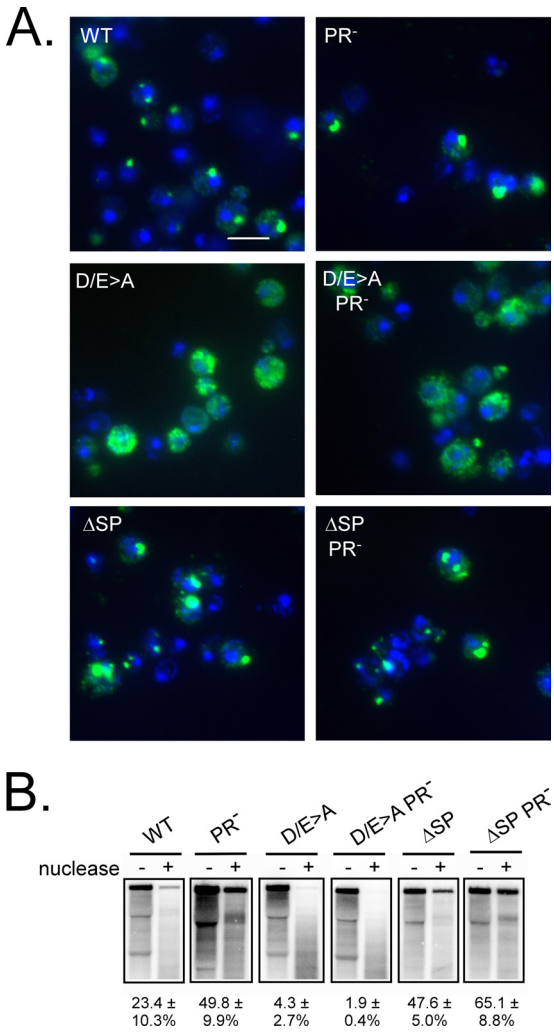

FIG. 4. Focus formation and RNA packaging by D/E → A and ΔSP mutant Ty3 elements. Cells expressing wt or mutant derivative Ty3 were induced by growth in SG Ura$^-$ medium for 6 h. (A) The subcellular localization of Ty3 Gag3 protein was monitored by indirect immunofluorescence using rabbit polyclonal anti-Ty3 CA and secondary antibody mouse monoclonal anti-rabbit conjugated to Alexa Fluor-488 fluorochrome. This signal was detected with an FITC filter and pseudo-colored green. DAPI nuclear staining was pseudo-colored blue. Bar, 5 μm. (B) Determination of RNA packaging. Nuclease protection of Ty3 RNA by particle encapsidation was monitored after the addition of TurboNuclease. An *in vitro* transcribed, truncated Ty3 RNA was added to extracts prior to nuclease treatment to monitor digestion of unpackaged Ty3 RNA. Packaged Ty3 RNA is expressed as the fraction of undigested Ty3 RNA in the treated sample over total Ty3 RNA present in the control, untreated sample. The percentages of RNA packaged were averaged from three independent assays performed for each mutant.

expressing wt Ty3. Together these results indicated that SP is not essential for formation of Ty3 assembly foci but that if SP is present, replacing the charged residues within it disrupts focus formation.

Ty3 NC zinc finger mutants do not form cytoplasmic foci and are defective in packaging Ty3 genomic RNA. NC zinc finger mutant Gag3 concentrates in the nuclei (26), presumably because it fails to recognize genomic Ty3 RNA. The retention in

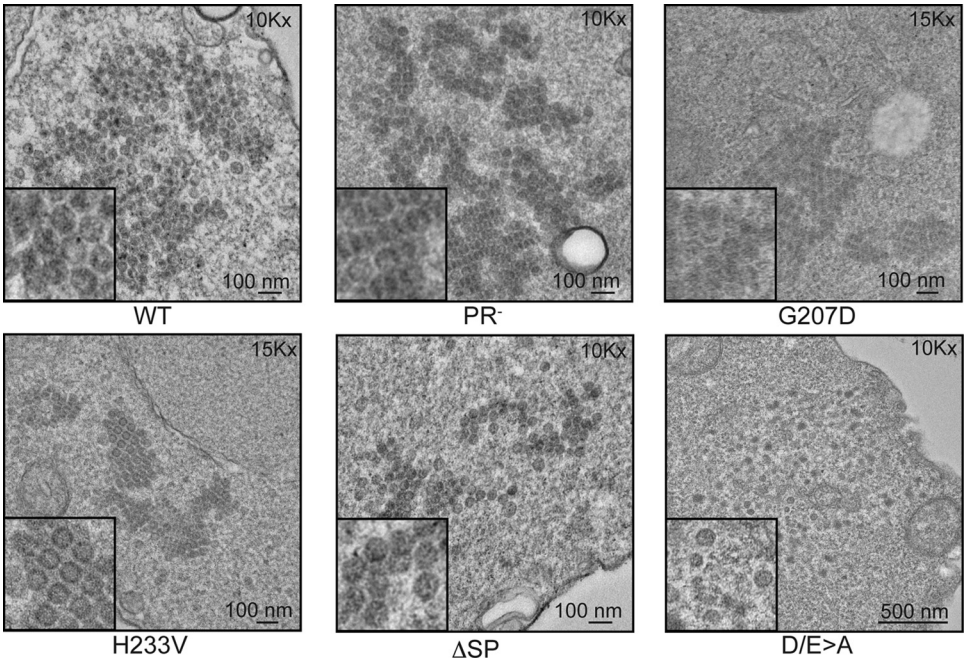

FIG. 5. Transmission electron microscopy of Ty3 VLPs. Cells transformed with wt Ty3 and mutant derivatives were grown in SG medium for 6 h to allow Ty3 expression. Cells were harvested and processed for imaging as described in Materials and Methods. Cells were imaged at 100 kV. Magnification (e.g., 10Kx, magnification of ×10,000) and scale bars are indicated in the individual panels. Insets are at a magnification of ×2.5 of the original images.

the cytoplasm of the D/E → A mutant Gag3 suggested that the Gag3 NC domain engages RNA. Because retrotransposons are intracellular, RNA packaging must be assessed using a nuclease protection assay to remove contaminating unpackaged Ty3 RNA. Nuclease protection assays were performed to test RNA protection of the D/E → A and ΔSP mutants. In extracts of cells that expressed wt Ty3 for 8 h, 23.4 ± 10.3% of Ty3 RNA was protected from nuclease digestion, and protection was greater for the PR$^-$ mutant (Fig. 4B). However, extracts of cells expressing the D/E → A or the PR$^-$ derivative did not show significant protection of Ty3 RNA. In contrast, the ΔSP mutant extracts protected a higher fraction of RNA than the wt, and this was further enhanced in the PR$^-$ derivative. These results suggest that the D/E → A mutant failed prior to or at the stage of protein condensing around the genomic RNA. The ΔSP mutant not only assembled but also formed particles which were more resistant to nuclease than wt particles. Because the level of protection afforded by the ΔSP PR$^-$ mutant was higher than the level of protection by the PR$^-$ mutant, this difference is not likely to be attributable to differences in RNase H activity.

SP processing mutants have aberrant particle morphologies. The ability of G207D and ΔSP Ty3 mutants to undergo proteolytic processing, produce NC, and generate cDNA contrasted with the defective retrotransposition of these mutants. This suggested that SP-NC cleavage is required for cDNA synthesis but that both SP and CA-SP cleavage have roles subsequent to cDNA synthesis. One possibility would be that they function to facilitate uncoating, thus making cDNA accessible for integration. TEM and AFM were utilized to examine Ty3 wt and mutant particles for differences in particle structure.

When examined by TEM, cells expressing Ty3 show large clusters of VLPs (Fig. 5), corresponding to the assembly foci visualized by indirect immunofluorescence (Fig. 4A). The PR$^-$ mutant was examined to exemplify VLPs in the immature state. In cells expressing the PR$^-$ mutant, particles occurred in chains and appeared to be overlapping like flattened VLP doublets with outer, electron-dense regions. In contrast, cells expressing wt Ty3 had more irregularly sized and distributed VLPs with electron-dense centers, representing the condensed ribonucleoprotein cores. Cells expressing the G207D mutant contained clusters of tightly packed VLPs in disordered arrays. Consistent with the ability of this mutant to produce mature NC, many particles had electron-dense centers. The H233V mutant particles were most similar to those of the PR$^-$ mutant in that VLPs lacked electron-dense centers and were in a highly ordered matrix. This phenotype was consistent with undetectable Gag3 processing. However, these particles lacked the compressed overlapping appearance of the PR$^-$ mutant, suggesting a difference possibly related to Gag3-Pol3 processing. Inspection of cells expressing the ΔSP mutant showed that this mutant formed particles but that these particles were elongated and appeared connected in chains rather than large orderly matrices. Electron-dense regions were more unevenly distributed for wt and G207D. Overall, these results showed that maturation of NC, rather than processing of CA-SP or any function of SP, is the key step to allow electron-dense core formation. In these mutants, this property correlated with production of cDNA. Out of over 100 cells expressing the D/E →

A mutant, relatively few showed evidence of particle formation. However, in a fraction of the samples, low-density collections of partially condensed particles were observed (Fig. 5). These structures had a bubbly, uneven appearance and lacked the integrity of wt particles.

AFM visualization of particle surfaces. TEM showed that the G207D mutation, which disrupted CA-SP but not SP-NC processing, was associated with VLPs having dense centers and tightly packed VLP clusters. This observation, coupled with the ability of this mutant to make cDNA but an inability to retrotranspose, raised the possibility that processing of SP affects particle uncoating. AFM was previously used to examine the external structure of Ty3 particles (25). This analysis showed that wt VLPs are heterogeneous but that PR$^-$ mutants are relatively uniform, with capsomere features characterized by both pentagonal and hexagonal symmetry. If CA-SP processing is required to achieve the heterogeneous state of wt particles, then the individual G207D and H233V mutants and the double mutant would have regular surface structures, similar to the structure of the PR$^-$ mutant. AFM analysis showed that the single mutants had regular structures that did not change significantly with inactivation of PR (Fig. 6). G207D H233V mutant particles appeared to be irregular, but mutant G207D H233V PR$^-$ particles were more regular. Although this result did not conform to the anticipated appearance of unprocessed particles, it could also be that the G207D H233V mutations destabilized particles through another mechanism. This interpretation is supported by the observation that this mutant produced less IN than the other mutants and that PR inactivation increased the amount of Gag3-Pol3 (Fig. 3A, lanes 7 and 8). Despite the apparent abundance of ΔSP mutant protein, Ty3 protein in the VLP fraction was significantly reduced compared to similar preparations from cells expressing wt Ty3 (data not shown). Ordered particles were observed in the absence or presence of the PR$^-$ mutation.

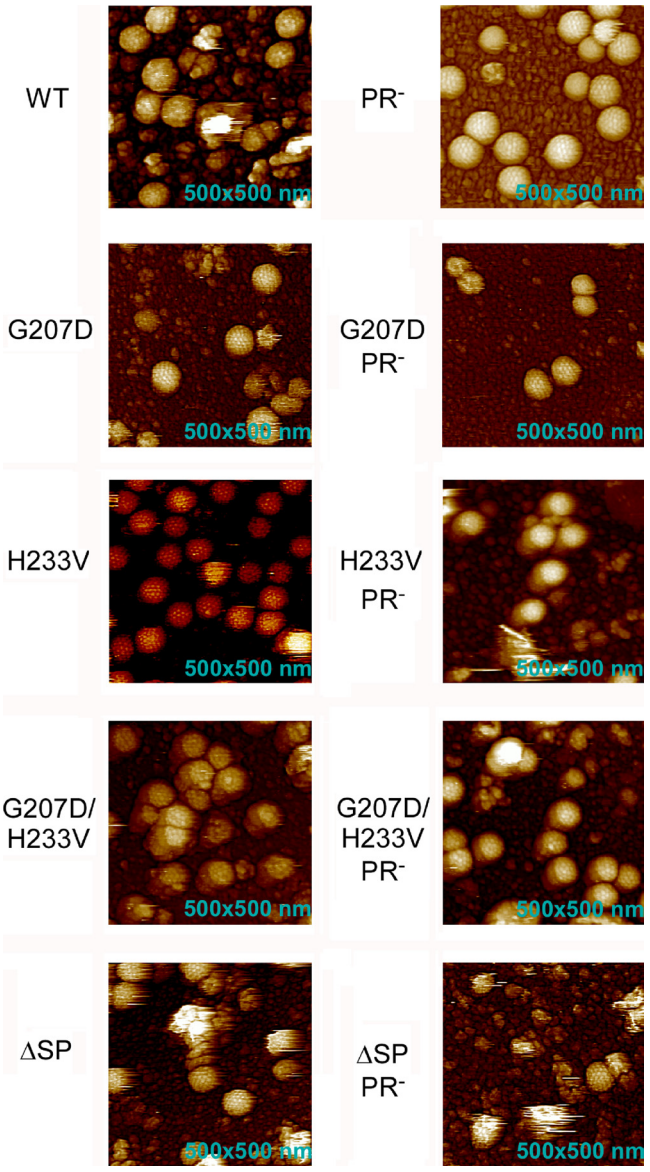

FIG. 6. Atomic force microscopy of Ty3 SP processing mutant VLPs. Yeast cells were induced for Ty3 expression by growth of transformants in SG Ura$^-$ medium for 18 h. Cells were harvested, and WCE were fractionated by velocity sedimentation over sucrose step gradients (see data at https://webfiles.uci.edu/sbsandme/lab/). VLPs were collected at the 30%-70% interface and processed for AFM.

DISCUSSION

Some retrovirus Gag proteins contain an SP domain between CA and NC domains. Where it has been studied, this domain is important for assembly and core condensation. Retrotransposons undergo intracellular assembly and replication. The existence of a SP domain in the Ty3 retrotransposon allowed exploration of the role of this domain in retrotransposition. We found that the negative charge of Ty3 SP is essential for assembly of the normal amount of particles. However, Ty3 particles can be assembled in the absence of this domain. Our results showed that these particles produce about half the amount of cDNA produced by wt particles but are 16-fold less active for transposition. Thus, Ty3 SP must also play a critical postreplication role in retrotransposition.

Cleavage of SP is context dependent and ordered. wt Gag3 is processed into major CA-SP, CA, and NC species. The current study showed that processing within the Pol3 domain of Gag3-Pol3 requires assembly but is independent of Gag3 processing. Mutations that disrupted Gag3 processing had nonreciprocal effects. The G207D mutation, which disrupted processing at CA-SP, did not interfere with production of NC. In contrast, the H233V mutation at the SP-NC junction blocked processing at that cleavage site and also interfered with CA-SP processing. Although this could result from effects of the H233V mutation on the overall folding of Gag3, the fact that the H233V mutant was competent for particle formation, and even Gag3-Pol3 processing of IN, argued against this mutation having a long-range, deleterious effect on Gag3 folding. A simpler explanation, consistent with the presence of the CA-SP intermediate in extracts of cells expressing wt Ty3, is that processing is ordered, with the SP-NC cleavage not only preceding CA-SP cleavage but also potentially required for that cleavage. A requirement for cleavage of Ty3 SP-NC prior to CA-SP would make it similar to the processing of HIV-1 Gag at the SP1-NC junction prior to processing at the CA-SP1

junction (34) although the Gag of that retrovirus has additional intervening processing not represented in the simpler Gag3.

The fact that multiple changes at the processing site, particularly introduction of beta-branched amino acids predicted to be disfavored at PR cleavage junctions, failed to completely block processing in the vicinity of SP suggests that context contributes significantly to cleavage in this region. However, it could also be the case that PR is insensitive to these changes, as has been observed in the case of some retroviruses (41). Additionally, the presence of minor cleavage products suggested that other sites within SP might serve as alternative cleavage sites in the absence of the preferred site, as has been demonstrated for HIV-1 (23, 45).

SP contributes to condensation and uncoating of the Ty3 particle. Deletion of Ty3 SP and neutralization of the SP charge bias led to distinct phenotypes that provided insights into the functions of Ty3 SP. One of the earliest events after induction of Ty3 expression is the appearance of cytoplasmic foci of Ty3 protein and RNA and P body components (2). These foci formed in cells expressing ΔSP, but both foci and particles were underrepresented in cells expressing the D/E → A mutant. The particles that formed differed from those formed by wt Ty3 and were heterogeneous in size and shape. Although this could result from gross misfolding of Gag3, some other mutations that interfered with assembly destabilized Gag3 (26, 27), but the D/E → A mutation did not significantly reduce amounts of Gag3.

We propose that domains of Ty3 Gag3 change conformation during assembly and that mutations affecting SP and NC charge or binding to RNA disrupt this progression. Taylor et al. (42) used nuclear magnetic resonance (NMR) to analyze a fragment comprised of the RSV CA C-terminal domain (CTD)-SP-NC in the presence and absence of oligonucleotides. On the basis of these experiments, they proposed that the CA CTD and neighboring SP interact to antagonize multimer formation in the absence of RNA but that binding of RNA by NC disrupts this conformation, allowing initiation of assembly. A related sequence of events could occur during Ty3 assembly. An intramolecular interaction between the acidic SP domain and the basic NC domain could limit intermolecular CA domain interactions prior to the NC domain binding RNA (Fig. 7). Upon binding of RNA, the basic NC domain might be more available for intermolecular interactions with SP, thereby allowing intermolecular interactions of CA and even promoting multimerization of Gag3 on the RNA. An intermolecular interaction involving NC would be analogous to the model proposed for human T-cell lymphotropic virus type 1. That NC has an acidic domain, which NMR studies have shown stabilizes NC binding to RNA. Stabilization is proposed to be mediated by intermolecular interactions between the acidic and basic domains of NC, which favor multimerization on the RNA (36). The Ty3 model would differ from that model in that the acidic domain of SP, rather than NC, would provide intermolecular interactions that promote assembly.

The defective assembly of the Gag3 mutant with neutral SP is in contrast to the foci and particles formed by the ΔSP mutant and visualized by TEM and AFM. Initially, the ability of ΔSP to form particles might seem at odds with the idea that intermolecular SP-NC interactions promote assembly. However, it is possible that in addition to promoting multimerization, the negative charge on SP is important for folding of a spacer domain into Gag3 multimers. If SP is lacking, NC domain binding to RNA might be sufficient to promote enough CA intermolecular interaction to support Gag3 multimerization.

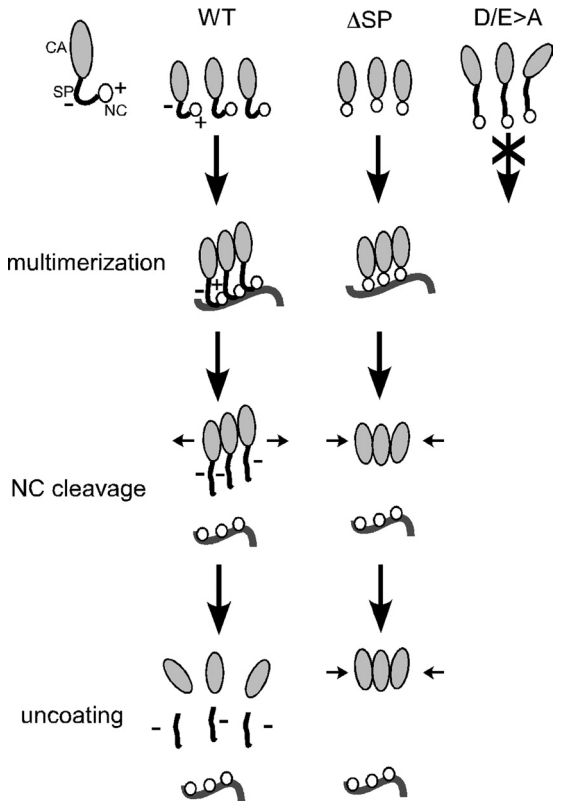

FIG. 7. Speculative model for SP contribution to Ty3 VLP morphogenesis. During assembly, wt Ty3 VLP formation occurs in the presence of the native SP domain, which contains acidic residues that interact with basic regions of NC to limit multimerization. After NC binding to genomic RNA, intermolecular interactions of these domains can occur and foster multimerization. Without interference by SP, ΔSP Gag3 can assemble on genomic RNA, but this process is inefficient. D/E → A Ty3 Gag3 includes an extended, uncharged SP domain that interferes with Gag3 multimerization, causing assembly to fail. Proteolytic cleavage of wt Ty3 allows for condensation of NC and RNA. The remaining CA-SP intermediate has a negatively charged SP which acts as a spring to destabilize the CA-SP shell and allow uncoating. ΔSP Ty3 Gag3 is processed into NC and CA but lacks the negatively charged SP domain, and so does not uncoat efficiently, resulting in a late-stage block to retrotransposition.

Ty3 SP is apparently not essential for gross assembly of particles or even cDNA synthesis. The ΔSP Gag3 protected RNA from nuclease digestion to a greater extent than wt Ty3 Gag3, suggesting that it forms compact particles, and TEM showed that G207D and H233V Ty3 produced relatively uniform VLPs compared to wt. However, the ΔSP mutant was profoundly defective for retrotransposition, underscoring the importance of SP. Mutant G207D was similar to ΔSP in that it produced NC and significant levels of cDNA but failed to retrotranspose. Together, the ΔSP and G207D phenotypes argue that SP must be both present and

cleaved from CA to allow some step in morphogenesis during or subsequent to reverse transcription. One candidate for such a step would be rearrangement of CA to allow uncoating. For example, a negatively charged SP domain could destabilize a CA-SP/CA-SP network to promote uncoating. Sequential roles for SP in compaction and uncoating of Gag3 are consistent with the molecular phenotypes of CA, SP, and NC mutants but are not yet demonstrated by biophysical measurements or crystallography.

Summary. We speculate that Ty3 SP acts as a molecular spring, promoting first Gag3 assembly and then VLP uncoating. In the first stage, the acidic SP domain of Gag3 has intramolecular interactions with the basic NC domain. In the second stage, the NC domain binds RNA nonspecifically, and intermolecular interactions occur between it and the SP domain. Such interactions could support multimerization of Gag3 on the RNA, thereby promoting CA-CA interactions. In a third phase, which could overlap with reverse transcription, the negatively charged SP domain destabilizes CA-SP interactions, allowing disassembly to a stage that releases an integration-competent form of cDNA. A role for SP in assembly through RNA binding and multimerization and then in dissociation may have evolved in a retrotransposon in order to allow differential regulation of events required for concentration of structural subunits, assembly of a stable particle, and reverse transcription and events involved in uncoating.

ACKNOWLEDGMENTS

This research was supported in whole or in part by funds from the National Institutes of Health (NIH), Public Health Service grant GM33281 to S.S., NSF EF-0330786, NIH CA112560, and NIH LM-07443-01 to P.B., GM58868 to A.M., and NCI, NIH, contract HHSN26120080001E to K.N.

We thank W. E. Robinson for providing the HIV-1 SP1 DNA sequence and B. Irwin for technical support and helpful discussions. We thank the reviewers for helpful suggestions.

REFERENCES

1. **Accola, M. A., S. Hoglund, and H. G. Gottlinger.** 1998. A putative alpha-helical structure which overlaps the capsid-p2 boundary in the human immunodeficiency virus type 1 Gag precursor is crucial for viral particle assembly. J. Virol. **72:**2072–2078.
2. **Beliakova-Bethell, N., et al.** 2006. Virus-like particles of the Ty3 retrotransposon assemble in association with P-body components. RNA **12:**94–101.
3. **Beliakova-Bethell, N., et al.** 2009. Ty3 nuclear entry is initiated by VLP docking on GLFG nucleoporins. J. Virol. **83:**11914–11925.
4. **Bohmova, K., et al.** 2010. Effect of dimerizing domains and basic residues on in vitro and in vivo assembly of Mason-Pfizer monkey virus and human immunodeficiency virus. J. Virol. **84:**1977–1988.
5. **Bryson, K., et al.** 2005. Protein structure prediction servers at University College London. Nucleic Acids Res. **33:**W36–W38.
6. **Cheslock, S. R., et al.** 2003. Charged assembly helix motif in murine leukemia virus capsid: an important region for virus assembly and particle size determination. J. Virol. **77:**7058–7066.
7. **Craven, R. C., A. E. Leure-duPree, C. R. Erdie, C. B. Wilson, and J. W. Wills.** 1993. Necessity of the spacer peptide between CA and NC in the Rous sarcoma virus Gag protein. J. Virol. **67:**6246–6252.
8. **Fingerman, E. G., P. G. Dombrowski, C. A. Francis, and P. D. Sniegowski.** 2003. Distribution and sequence analysis of a novel Ty3-like element in natural *Saccharomyces paradoxus* isolates. Yeast **20:**761–770.
9. **Ganser-Pornillos, B. K., M. Yeager, and W. I. Sundquist.** 2008. The structural biology of HIV assembly. Curr. Opin. Struct. Biol. **18:**203–217.
10. **Gross, I., et al.** 2000. A conformational switch controlling HIV-1 morphogenesis. EMBO J. **19:**103–113.
11. **Guo, X., J. Hu, J. B. Whitney, R. S. Russell, and C. Liang.** 2004. Important role for the CA-NC spacer region in the assembly of bovine immunodeficiency virus Gag protein. J. Virol. **78:**551–560.
12. **Guo, X., and C. Liang.** 2005. Opposing effects of the M368A point mutation and deletion of the SP1 region on membrane binding of human immunodeficiency virus type 1 Gag. Virology **335:**232–241.
13. **Guo, X., A. Roldan, J. Hu, M. A. Wainberg, and C. Liang.** 2005. Mutation of the SP1 sequence impairs both multimerization and membrane-binding activities of human immunodeficiency virus type 1 Gag. J. Virol. **79:**1803–1812.
14. **Guo, X., et al.** 2005. The R362A mutation at the C-terminus of CA inhibits packaging of human immunodeficiency virus type 1 RNA. Virology **343:**190–200.
15. **Hansen, L. J., D. L. Chalker, K. J. Orlinsky, and S. B. Sandmeyer.** 1992. Ty3 GAG3 and POL3 genes encode the components of intracellular particles. J. Virol. **66:**1414–1424.
16. **Hansen, L. J., D. L. Chalker, and S. B. Sandmeyer.** 1988. Ty3, a yeast retrotransposon associated with tRNA genes, has homology to animal retroviruses. Mol. Cell. Biol. **8:**5245–5256.
17. **Irwin, B., et al.** 2005. Retroviruses and yeast retrotransposons use overlapping sets of host genes. Genome Res. **15:**641–654.
18. **Kaye, J. F., and A. M. Lever.** 1998. Nonreciprocal packaging of human immunodeficiency virus type 1 and type 2 RNA: a possible role for the p2 domain of Gag in RNA encapsidation. J. Virol. **72:**5877–5885.
19. **Keller, P. W., M. C. Johnson, and V. M. Vogt.** 2008. Mutations in the spacer peptide and adjoining sequences in Rous sarcoma virus Gag lead to tubular budding. J. Virol. **82:**6788–6797.
20. **Kinsey, P. T., and S. B. Sandmeyer.** 1995. Ty3 transposes in mating populations of yeast: a novel transposition assay for Ty3. Genetics **139:**81–94.
21. **Kirchner, J., and S. Sandmeyer.** 1993. Proteolytic processing of Ty3 proteins is required for transposition. J. Virol. **67:**19–28.
22. **Kirchner, J., and S. B. Sandmeyer.** 1996. Ty3 integrase mutants defective in reverse transcription or 3′-end processing of extrachromosomal Ty3 DNA. J. Virol. **70:**4737–4747.
23. **Krausslich, H. G., M. Facke, A. M. Heuser, J. Konvalinka, and H. Zentgraf.** 1995. The spacer peptide between human immunodeficiency virus capsid and nucleocapsid proteins is essential for ordered assembly and viral infectivity. J. Virol. **69:**3407–3419.
24. **Krishna, N. K., S. Campbell, V. M. Vogt, and J. W. Wills.** 1998. Genetic determinants of Rous sarcoma virus particle size. J. Virol. **72:**564–577.
25. **Kuznetsov, Y. G., M. Zhang, T. M. Menees, A. McPherson, and S. Sandmeyer.** 2005. Investigation by atomic force microscopy of the structure of Ty3 retrotransposon particles. J. Virol. **79:**8032–8045.
26. **Larsen, L. S., et al.** 2008. Ty3 nucleocapsid controls localization of particle assembly. J. Virol. **82:**2501–2514.
27. **Larsen, L. S., et al.** 2007. Ty3 capsid mutations reveal early and late functions of the amino-terminal domain. J. Virol. **81:**6957–6972.
28. **Li, F., et al.** 2003. PA-457: a potent HIV inhibitor that disrupts core condensation by targeting a late step in Gag processing. Proc. Natl. Acad. Sci. U. S. A. **100:**13555–13560.
29. **Lin, J. H., and H. L. Levin.** 1998. Reverse transcription of a self-primed retrotransposon requires an RNA structure similar to the U5-IR stem-loop of retroviruses. Mol. Cell. Biol. **18:**6859–6869.
30. **Menees, T. M., and S. B. Sandmeyer.** 1994. Transposition of the yeast retrovirus like element Ty3 is dependent on the cell cycle. Mol. Cell Biol. **14:**8229–8240.
31. **Misumi, S., et al.** 1997. The $p2^{gag}$ peptide, AEAMSQVTNTATIM, processed from HIV-1 $Pr55^{gag}$ was found to be a suicide inhibitor of HIV-1 protease. Biochem. Biophys. Res. Commun. **241:**275–280.
32. **Misumi, S., et al.** 2004. Blocking of human immunodeficiency virus type-1 virion autolysis by autologous $p2^{gag}$ peptide. J. Biochem. **135:**447–453.
33. **Morikawa, Y., D. J. Hockley, M. V. Nermut, and I. M. Jones.** 2000. Roles of matrix, p2, and N-terminal myristoylation in human immunodeficiency virus type 1 Gag assembly. J. Virol. **74:**16–23.
34. **Pettit, S. C., N. Sheng, R. Tritch, S. Erickson-Viitanen, and R. Swanstrom.** 1998. The regulation of sequential processing of HIV-1 Gag by the viral protease. Adv. Exp. Med. Biol. **436:**15–25.
35. **Pettit, S. C., et al.** 1991. Analysis of retroviral protease cleavage sites reveals two types of cleavage sites and the structural requirements of the P1 amino acid. J. Biol. Chem. **266:**14539–14547.
36. **Qualley, D. F., et al.** 2010. C-terminal domain modulates the nucleic acid chaperone activity of human T-cell leukemia virus type 1 nucleocapsid protein via an electrostatic mechanism. J. Biol. Chem. **285:**295–307.
37. **Rumlova, M., T. Ruml, J. Pohl, and I. Pichova.** 2003. Specific in vitro cleavage of Mason-Pfizer monkey virus capsid protein: evidence for a potential role of retroviral protease in early stages of infection. Virology **310:**310–318.
38. **Russell, R. S., et al.** 2003. Effects of a single amino acid substitution within the p2 region of human immunodeficiency virus type 1 on packaging of spliced viral RNA. J. Virol. **77:**12986–12995.
39. **Sandmeyer, S. B., M. Aye, and T. Meenes.** 2002. Ty3, a position-specific, Gypsy-like element in *Saccharomyces cerevisiae*, p. 663–683.*In* N. L. Craig, et al. (ed.), Mobile DNA II. ASM Press, Washington DC.
40. **Scarlata, S., and C. Carter.** 2003. Role of HIV-1 Gag domains in viral assembly. Biochim. Biophys. Acta **1614:**62–72.
41. **Schatz, G., I. Pichova, and V. M. Vogt.** 1997. Analysis of cleavage site

mutations between the NC and PR Gag domains of Rous sarcoma virus. J. Virol. **71:**444–450.
42. **Taylor, G. M., L. Ma, V. M. Vogt, and C. B. Post.** 2010. NMR relaxation studies of an RNA-binding segment of the Rous sarcoma virus gag polyprotein in free and bound states: a model for autoinhibition of assembly. Biochemistry **49:**4006–4017.
43. **Teysset, L., V. D. Dang, M. K. Kim, and H. L. Levin.** 2003. A long terminal repeat-containing retrotransposon of *Schizosaccharomyces pombe* expresses a Gag-like protein that assembles into virus-like particles which mediate reverse transcription. J. Virol. **77:**5451–5463.
44. **von Schwedler, U. K., et al.** 1998. Proteolytic refolding of the HIV-1 capsid protein amino-terminus facilitates viral core assembly. EMBO J. **17:**1555–1568.
45. **Wiegers, K., et al.** 1998. Sequential steps in human immunodeficiency virus particle maturation revealed by alterations of individual Gag polyprotein cleavage sites. J. Virol. **72:**2846–2854.
46. **Williams, J. G., and W. B. Gratzer.** 1971. Limitations of the detergent-polyacrylamide gel electrophoresis method for molecular weight determination of proteins. J. Chromatogr. **57:**121–125.
47. **Wright, E. R., et al.** 2007. Electron cryotomography of immature HIV-1 virions reveals the structure of the CA and SP1 Gag shells. EMBO J. **26:**2218–2226.